This article is published as part of the *Dalton Transactions* themed issue entitled:

Coordination chemistry in the solid state

Guest Editor Russell E. Morris

Published in Issue 14, Volume 41 of *Dalton Transactions*

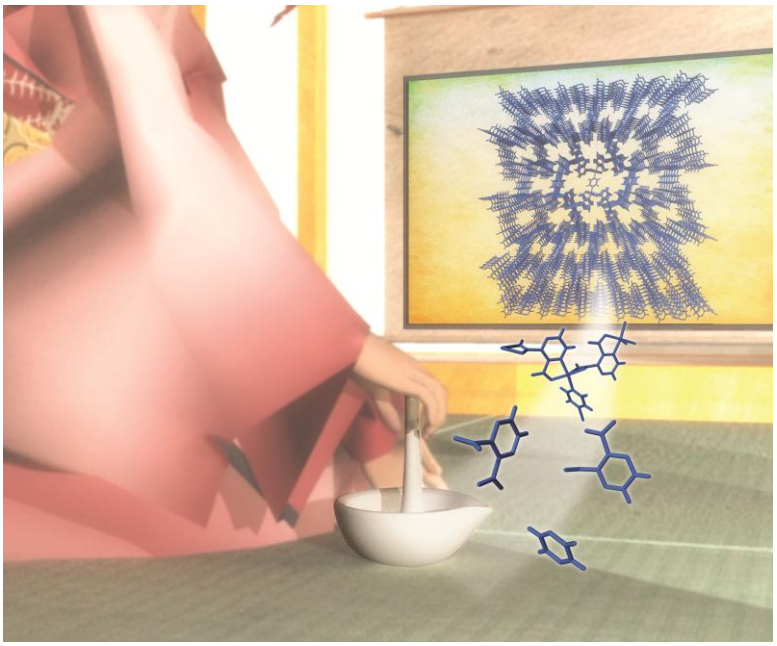

Articles in this issue include:

Communications

Highly oriented surface-growth and covalent dye labeling of mesoporous metal–organic frameworks
Florian M. Hinterholzinger, Stefan Wuttke, Pascal Roy, Thomas Preuße, Andreas Schaate, Peter Behrens, Adelheid Godt and Thomas Bein

Papers

Supramolecular isomers of metal–organic frameworks: the role of a new mixed donor imidazolate-carboxylate tetradentate ligand
Victoria J. Richards, Stephen P. Argent, Adam Kewley, Alexander J. Blake, William Lewis and Neil R. Champness

Hydrogen adsorption in the metal–organic frameworks Fe_2(dobdc) and $Fe_2(O_2)$(dobdc)
Wendy L. Queen, Eric D. Bloch, Craig M. Brown, Matthew R. Hudson, Jarad A. Mason, Leslie J. Murray, Anibal Javier Ramirez-Cuesta, Vanessa K. Peterson and Jeffrey R. Long

Visit the *Dalton Transactions* website for the latest cutting inorganic chemistry
www.rsc.org/publishing/journals/dt/

Dalton Transactions

Dynamic Article Links

Cite this: *Dalton Trans.*, 2012, **41**, 4036

www.rsc.org/dalton

PAPER

Synthesis of quinolines *via* Friedländer reaction catalyzed by CuBTC metal–organic-framework

Elena Pérez-Mayoral,[a,b] Zuzana Musilová,[b] Barbara Gil,[c] Bartosz Marszalek,[c] Miroslav Položij,[d] Petr Nachtigall[d] and Jiri Čejka*[b]

Received 19th October 2011, Accepted 9th December 2011
DOI: 10.1039/c2dt11978a

Friedländer condensation between 2-aminoaryl ketones and different carbonyl compounds, catalyzed by CuBTC was investigated by a combination of various experimental techniques and by density functional theory based modelling. CuBTC exhibiting hard Lewis acid character showed highly improved catalytic activity when compared with other molecular sieves showing high concentraion of Lewis acid sites, *e.g.* in BEA and (Al)SBA-15. Polysubstituted quinolines were synthesized *via* a Friedländer reaction catalyzed by CuBTC under the solvent-free conditions. High concentration of active sites in CuBTC together with the concerted effect of a pair of adjacent Cu^{2+} coordinatively unsaturated active sites are behind a very high quinoline yield reached within a short reaction time. Results reported here make CuBTC a promising catalyst for other Lewis acid-promoted condensations, including those leading to biologically active compounds with a particular relevance for the pharmaceutical industry. The mechanism of a catalyzed Friedländer reaction investigated computationally is also reported.

1. Introduction

Metal–Organic-Frameworks (MOFs) are considered to be one of the most fascinating groups of materials due to their structural and chemical features and potential applications in areas like optoelectronic devices[1] and sensors,[2] storage and separation of gases,[3] and even medical imaging and drug delivery.[4] Furthermore, crystalline MOFs, possess large specific surface areas and uniform size distribution of the channels, which make them promising for heterogeneous catalysis.[5] Channel systems of MOFs show a strictly ordered geometry, which could allow for their use in size and shape selective catalysis, this type of catalysis being up-to-now reported exclusively for zeolites.[6] In contrast to zeolites, MOFs are formed in principle from an "infinite" set of building blocks and metals making them potentially more versatile than zeolites.[7]

In the green chemistry context, we investigate the almost unexplored catalytic behaviour of MOF materials, particularly CuBTC (Basolite™ C300). The presence of metals in the MOFs structure acting as unsaturated coordination sites enables their application as catalysts for oxidation–reduction reactions. In this way, CuBTC and Fe(BTC) have been reported as efficient catalysts in the oxidation of *p*-benzoquinone,[8] and benzylic compounds.[9] CuBTC is a 3D porous MOF with a zeolite-like structure,[10] possessing a marked hard Lewis acid character.[11] CuBTC was reported as catalytically active in the cyanosilylation of aldehydes,[12] and recently in the cyclopropanation reaction of olefins with diazoacetate esters.[13]

More recently, we reported on Basolite™ C300, CuBTC, as an efficient and environmentally-friendly catalyst for the Friedländer reaction between 2-aminobenzophenones and acetylacetone under mild reaction conditions.[14] Our studies demonstrated that the annulation is promoted by Lewis acid sites located over metallic centers in CuBTC. This MOF was proposed as a novel catalyst for this transformation with improved catalytic properties when related to molecular sieves typically exhibiting Lewis acidity, H-BEA and (Al)SBA-15.[14,15]

Development of new and efficient catalysts for quinoline synthesis *via* a Friedländer reaction is currently an enormously interesting topic because this reaction is considered to be the most efficient and simple synthetic approach to prepare nitrogen heterocycles, quinoline systems, with important pharmacological activities.[16,17] Substitution in the quinoline ring system induces different effects on their biological activity. As examples, compounds **1a–b** were reported as antiparasitic agents[18] while tacrine-thiadiazolidinone hybrids **2** are acetylcholinesterase (AchE) inhibitors (Fig. 1).[19]

Among the heterogeneous catalysts reported for this annulation are Al_2O_3,[20] H_2SO_4/SiO_2,[21–23] $NaHSO_4/SiO_2$[24,25]

[a]*Departamento de Química Inorgánica y Química Técnica, Facultad de Ciencias, Paseo Senda del Rey 9, 28040 Madrid, Spain. E-mail: eperez@ccia.uned.es; Fax: (+34) 3989766; Tel: (+34) 3989047*
[b]*Department of Synthesis and Catalysis. J. Heyrovský Institute of Physical Chemistry, Academy of Sciences of the Czech Republic, v.v.i., Dolejškova 3, 182 23 Prague 8, Czech Republic. E-mail: jiri.cejka@jh-inst.cas.cz; Fax: (+)420-28658-2307; Tel: (+)420-26605-3795*
[c]*Department of Inorganic Chemistry, Faculty of Chemistry, Jagiellonian University, Ingardena 3, 30 060 Kraków, Poland. E-mail: gil@chemia.uj.edu.pl; Fax: (+48)12- 634-0515; Tel: (+)48-12663-2016*
[d]*Department of Physical and Macromolecular Chemistry, Faculty of Natural Sciences, Charles University, Albertov 2030, 120 00 Prague 2, Czech Republic. E-mail: petr.nachtigall@molecular.cz; Fax: (+)420-224919752; Tel: (+)420-221951289*

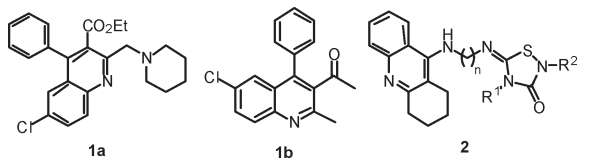

Fig. 1 Substituted quinolines with biological activity.

$HClO_4/SiO_2$,[26] silica gel-supported phosphomolybdic acid,[27] $KAl(SO_4)_2 12H_2O/SiO_2$,[28] sulfonated cellulose,[29] silica-propylsulfonic acid[30] and AlKIT-5.[31] In addition, we employed mesoporous materials as novel and efficient catalysts for the Friedländer condensation between 2-aminoaryl ketones and ethyl acetoacetate selectively leading to the corresponding quinolin-2(1*H*)-ones.[32] Synthesis of quinolines starting from aniline and different aldehydes catalyzed by H-BEA zeolite, under vapour phase conditions, was reported as well.[33]

This contribution is targeted to characterization and catalytic performance evaluation of CuBTC, in the synthesis of polysubstituted quinolines. It is a continuation of our preliminary results[14,15] offering the reaction scope as well as accompanied by the rationalization of the process by computational methods.

2. Results and discussion

2.1. Catalyst characterization

Table 1 shows the textural parameters of CuBTC. This MOF exhibited a specific surface area, S_{BET}, higher than the representative zeolite chosen for comparison. Furthermore, CuBTC showed large pore diameters and volumes up to almost 1 nm. This makes it a promising candidate as a catalyst for the synthesis of interesting compounds with industrial potential.

2.2. Lewis acidity of CuBTC

Lewis acidity of CuBTC arises from the presence of unsaturated Cu(II) centres. Lewis acidity, by analogy to zeolites, may be determined quantitatively by the adsorption of basic probe molecules.

At first, a new diagnostic band for coordinatively bonded pyridine had to be selected as the one typically used, with a maximum around 1450 cm^{-1}, overlapped with the native MOF bands. As the diagnostic one we chose the band at 1069 cm^{-1} assigned to ν_{18b} of CC out-of-plane vibrations. This band appears when pyridine is adsorbed on thermally treated MgO (all-Lewis-sites system), TiO_2 (mostly Lewis system) but is absent in HPW heteroacid (all-Brønsted-sites system), as presented in Fig. 2a. This assignment is in agreement with the literature data.[34]

Absorption coefficient of the 1069 cm^{-1} band was determined in experiments in which small, measured doses of pyridine were adsorbed in CuBTC activated at 423 K. Then, the dependence of intensity of the 1069 cm^{-1} band *vs.* the concentration of the absorbed pyridine is shown in Fig. 2b. The slope of this line was taken as the absorption coefficient of the 1069 cm^{-1} band. The average value for all experiments was 0.042 ± 0.0008 cm μmol^{-1}. On the basis of the determined absorption coefficient and intensity of the 1069 cm^{-1} band, the concentration of coordinatively bonded pyridine was determined as equal to 2.30 mmol g^{-1} for CuBTC activated at 473 K. It is worth mentioning that concentration of the Lewis sites was calculated for the weight of activated, partially dehydrated sample, determined from the activation experiments performed on the sorption balance. Fig. 3 shows that pyridine was not interacting with the residual water or OH groups. The bands of organic linker were also virtually unchanged after pyridine adsorption, independently of the temperature the MOF was activated. Thus, it is safe to assume that the stoichiometry of the pyridine interaction with the active centres was: one coordinatively unsaturated metal centre to one pyridine molecule.

Table 1 Textural parameters of catalysts under study

Catalyst	Si/Al ratio[a]	S_{BET}[b] ($m^2\ g^{-1}$)	D_{pore}[c] (nm)	V_{pore}[c] ($cm^3\ g^{-1}$)
Basolite™ C300	n.a.	1499	0.35; 0.50; 0.90	0.642
H-BEA	12.5	674	0.70 × 0.67	0.224

[a] Determined by X-ray fluorescence spectroscopy. [b] S_{BET} = BET surface area. [c] D_{pore} and V_{pore}, pore diameter and volume, respectively, calculated using BJH method.

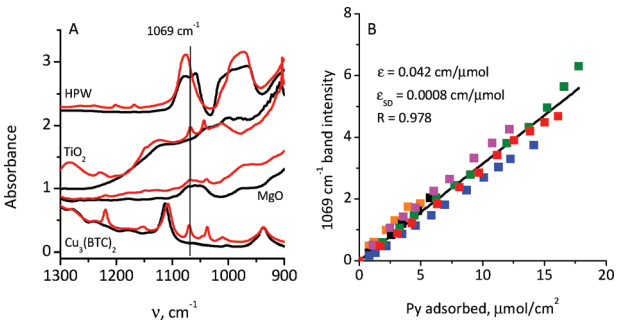

Fig. 2 A - IR spectra of pyridine adsorbed on HPW, MgO, TiO_2 and CuBTC, black lines – activated samples, red lines – after pyridine adsorption and consecutive evacuation for 15 min. B - dependence of the 1069 cm^{-1} band on the surface concentration of the adsorbed pyridine.

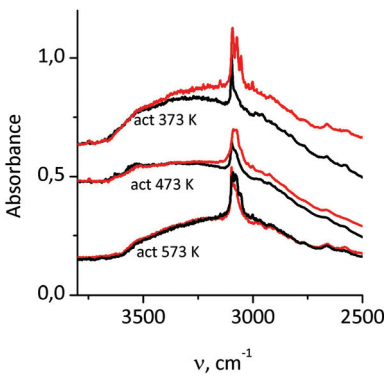

Fig. 3 IR spectra of CuBTC activated at 373, 473 and 573 K before (black spectra) and after (red spectra) pyridine adsorption at 373 K.

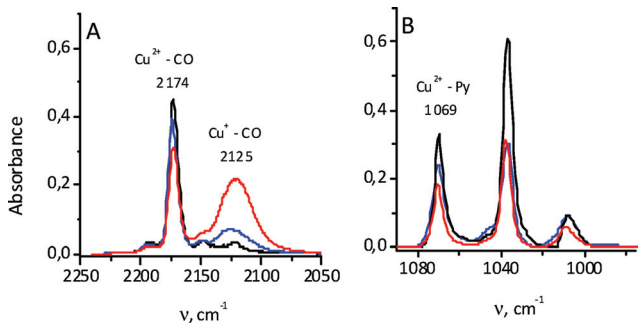

Fig. 4 IR spectra of CO (A) and pyridine (B) adsorbed on CuBTC activated at 373 (black), 473 (blue) and 573 K (red spectra).

In reality, a significant amount of water is still present in the activated sample. Moreover, water molecules are not being replaced by pyridine, thus at least a number of Cu^{2+} cations are 'shielded'. Adsorption of CO allows determination of the oxidation state of copper. In the case of CO adsorption in CuBTC, several bands are arising. Activation at increasing temperatures allows the assignment of two main maxima. The most intense band at 2174 cm^{-1} can be assigned to the Cu^{2+}–CO complex, the IR band rarely seen in zeolites, but observed in copper oxide systems.[35] The broad maximum at *ca.* 2125 cm^{-1}, appearing and growing at the expense of the band at 2174 cm^{-1} when the sample is activated at increasing temperatures, can be assigned to the Cu^{+}–CO moiety.[36]

To determine whether in addition to Cu^{2+} the Cu^{+} cations in CuBTC may also be active as Lewis sites, pyridine was adsorbed in samples activated at increasing temperatures (Fig. 3 and 4B). The number of Cu^{2+} centres, playing the role of Lewis acids, also decreased with increasing activation temperature, therefore it seems probable that Cu^{+} sites are not interacting with pyridine.

2.3. Catalytic performance

The catalytic activity of CuBTC was in the synthesis of quinoline **1b** by condensation of 2-amino-5-chlorobenzophenone (**3a**) with acetylacetone (**4**) (Scheme 1). At first, we carried out the condensation in the presence of CuBTC, under solvent-free conditions using an excess of ketone **4**, at 353 K.[14] Under these reaction conditions, compound **1b** was isolated with 92% yield after 2 h reaction time.

Fig. 5 depicts a time dependence of conversion for the condensation between compound **3a** and **4** catalyzed by CuBTC at different reaction temperatures. The reaction proceeds already at 343 K yielding compound **1b** in around 80% after 4 h. In addition, although final yield of **1b** when operating at the highest

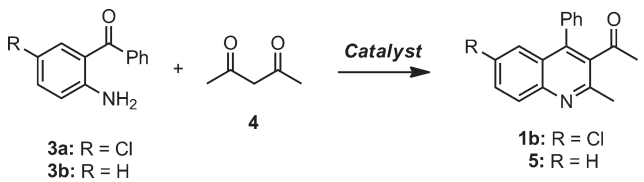

Scheme 1 Friedländer reaction between 2-aminoaryl ketones **3** and carbonyl compounds affording quinolines.

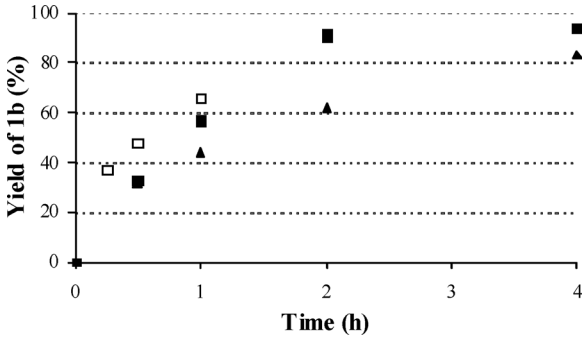

Fig. 5 Time conversion plot for the Friedländer reaction between 2-amino-5-chlorobenzophenone (**3a**) with acetylacetone (**4**) catalyzed by CuBTC at (□) 363 K (■) 353 K and (▲) 343 K.

reaction temperatures, 363 or 353 K, was almost in the same degree, it was considerably higher at the shortest reaction times when the reaction was carried out at 363 K. This feature can be observed in Table 2 showing the reaction rates for the condensation of **3a** with **4**, as a function of the temperature.

In order to compare the catalytic behaviour of CuBTC with zeolites and other catalysts, we selected the most reactive ketone,[14] 2-aminobenzophenone (**3b**) as a model reactant. For comparison, H-BEA was chosen due to our most recent results demonstrating that it was the most efficient zeolite catalyzing the Friedländer condensation.[15] Fig. 6 shows the yield of compound **5** over H-BEA at 363 K. Additionally, we studied the condensation of **3b** with **4** catalyzed by Cu-BEA. Fig. 6 confirms that CuBTC was the most efficient catalyst for the Friedländer reaction between compound **3a** and **4** as compared with H-BEA and its Cu analogue.

The condensation reaction leading to **5** is almost quantitative after 1.5 h when catalyzed by CuBTC while the same reaction gives only 75 and 52% yields over H-BEA and Cu-BEA, respectively.

Table 2 Reaction rates for the condensation of **3a** with **4**.

Sample	Act. 373 K	Act. 473 K	Act. 573 K
CuBTC	2.44	2.16	1.40

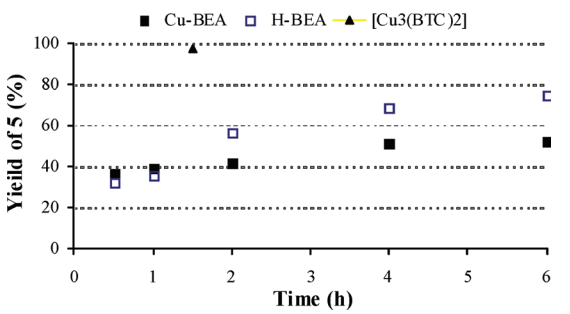

Fig. 6 Kinetic profiles for the Friedländer reaction between 2-aminobenzophenone (**3b**) with acetylacetone (**4**) catalyzed by (□) H-BEA (■) Cu-BEA and (▲) CuBTC.

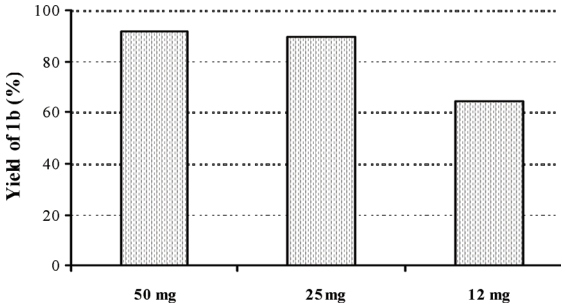

Fig. 7 Effect of catalyst amount in the condensation of **3a** with **4** catalyzed by CuBTC at 363 K.

Based on the molecular dimensions of the reactants and products,[14] when using CuBTC which has large pores, the process can take place inside or outside the channels, whereas in the case of zeolites the condensation probably proceeds mostly on the external surface. The highest concentration of Lewis acid sites in CuBTC, located over metallic centres, could be responsible for the great efficacy in the synthesis of quinoline **5**. Obviously, Brønsted acid sites in H-BEA may also be involved in the reaction. However, in the MOF catalyst under study, no Brønsted acid sites are present. To get a deeper insight, H-BEA zeolite was exchanged with Cu(II) leading to Cu-BEA. In the activated form of this zeolite, the copper atoms are usually Cu(I) as mentioned above. The lower yield of **5** in the reaction catalyzed by Cu-BEA could indicate that Cu(I) is mostly inactive in this reaction.

Therefore, we can infer that Lewis acid sites in CuBTC play a remarkable role in the annulation between **3** and **4** whereas both types of sites in zeolites, Brønsted and Lewis sites, contribute to the overall activity in the reaction.

Following our ongoing investigations we evaluated different catalyst amounts, in this case for the condensation of compounds **3a** and **4**. As it is seen from Fig. 7, the use of CuBTC in 8% (50 mg) and 4% (25 mg) afforded the compound **1b** with excellent yields, 92 and 90%, respectively. Decreasing amounts of the catalyst led to lower conversions to **1b**, therefore, the optimum catalyst amount should be kept at *ca.* 4% (25 mg).

In order to generalize the results of this study we carried out the Friedländer reaction of **3a** with different ketones with active methylene groups at the α-position (Scheme 2 and Table 3).

Thus, the reaction with cyclohexanone (**6**), a ketone less reactive than **4**, at 363 K over CuBTC, afforded quinoline **7** with quantitative yield after 5 h of the reaction time (Table 3; entry 2).

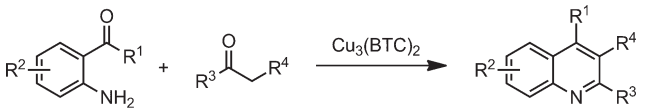

Scheme 2 Friedländer reaction between 2-aminoaryl ketones with different ketones.

In this case, the catalyst was recovered and analyzed by X-Ray Diffraction (XRD). Diffraction lines corresponding to the fresh and used CuBTC were observed although with a lower intensity, this circumstance is probably due to the small amount of the catalyst and the presence of reactants/products in the channel system. Therefore, CuBTC is a promising reusable catalyst.

We calculated the maximum catalyst TON (Table 3) for the condensation of **3a** with different ketones. Remarkably, TON increases when the reaction between **3a** and **4** was carried out using higher amounts of ketone **3a** (1 mmol) and a lower amount of catalyst (25 mg) as depicted in Fig. 7. The maximum values of TON and TOF were 2168 and 1084 h^{-1}, respectively. These values together XRD results indicate no early deactivation of the catalyst.

We also performed the condensation with dimedone (**8**) yielding compound **9** with 41% yield (Table 2; entry 3). This low yield might be caused by a lower solubility of this ketone in the reaction medium. Hence 1,2-dichloroethane (1 mL) was used as a solvent in order to facilitate the reaction. Finally, the reaction of **3a** with acetophenone (**10**) led to quinoline **11** with a moderate yield of 57%. A lower yield was the result of a lower reactivity of this ketone as compared with the others (Table 2; entry 4).

To complete the study we carried out the Friedländer reaction between acetylacetone (**4**) and 2-aminobenzophenones (Scheme 2 and Table 4). The influence of functional groups (carbonyl and amine) on the substitution in the aromatic ring was investigated (Table 4). Entries 1 and 2 in Table 4 have been previously commented on and the respective results shown in Fig. 6 and 7. On the other hand, the condensation of **12** with **4** yielded quinoline **13** in 67% yield after 7 h of the reaction (Table 3; entry 3). This result could be explained due to the weaker nucleophilic character of the amine group in compound **12** as compared with 2-aminoaryl ketone **3** with the nitro group present. While chlorine at the 5-position in **3a** produces a slight decrease in the yield of compound **1b** and hence a decrease in the reactivity, the presence of a nitro group, as a strongly electron-withdrawing group, reduces dramatically the reactivity of the compound **12**. Furthermore, we performed the reaction

Table 3 Friedländer reaction between 2-amino-5-chlorobenzophenone (**3a**) with different ketones, under solvent-free conditions and at 363 K, catalyzed by CuBTC

Entry	R^1	R^2	R^3	R^4	Ketone	Time (h)	Quinoline	Yield (%)	TON	TOF
1	Ph	Cl	CH_3	$COCH_3$	**4**	2	**1b**	92	554	272
2	Ph	Cl	$-(CH_2)_4-$		**6**	5	**7**	99	596	119
3	Ph	Cl	$-(CH_2)-C(CH_3)_2-CH_2-CO$		**8**	4	**9**	41[a]	246	61
4	Ph	Cl	Ph	H	**10**	15	**11**	57[b]	343	22

All the reactions were carried out using 0.5 mmol of 2-amino-5-chlorobenzophenone (**3a**). [a] Reaction was carried out in the presence of solvent (1,2-dichloroethane; 1 mL) at reflux and using the compounds **3a** and **8** in 1 : 1 ratio. [b] Reaction was performed at 393 K. Turnover number (TON) and Turnover frequency (TOF) are defined as TON = conversion (%) (mol(substrate))/mol (catalyst) while TOF = TON/time (h).

Table 4 Friedländer reaction between different 2-aminoaryl ketones with acetylacetone

Entry	R^1	R^2	R^3	R^4	2-aminoaryl ketone	Time (h)	Quinoline	Yield (%)
1	Ph	Cl	CH_3	$COCH_3$	**3a**	2	**1b**	92
2	Ph	H	CH_3	$COCH_3$	**3b**	1.5	**5**	97
3	Ph	NO_2	CH_3	$COCH_3$	**12**	7	**13**	67
4	Me	H	CH_3	$COCH_3$	**14**	4	**15**	64

All of the reactions were carried out using 0.5 mmol of the corresponding 2-aminoaryl ketone.

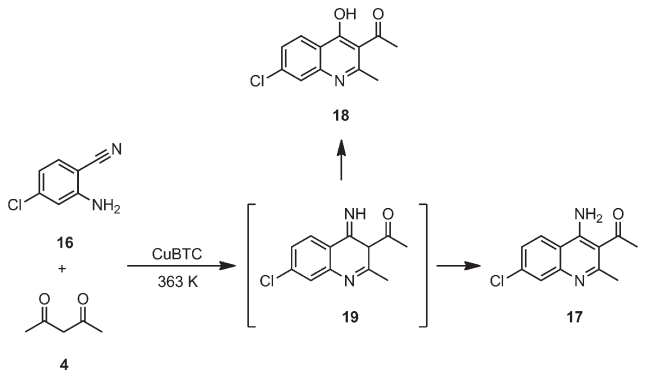

Scheme 3 Synthesis of 3-acetyl-4-amino-7-chloro-2-metilquinoline (**17**) starting from 2-amino-4-chlorobenzonitrile (**16**).

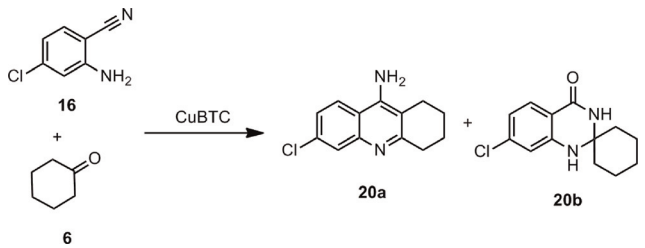

Scheme 4 Synthesis of tracrine derivatives.

between 2-aminoacetophenone (**14**) and acetylacetone (**4**) affording quinoline **15** in 64% yield for 4 h (Table 4; entry 4).

As mentioned, all MOFs consist of metallic centers and organic ligands. Although the channels of CuBTC seem accessible to reactant **14**, this substrate exhibited lower reactivity towards acetylacetone (**4**) than **1a**. We also observed this chemical behaviour when testing zeolites in the Friedländer reaction with both 2-aminoaryl ketones.[15] It could be rationalized that in the reactions with 2-aminobenzophenones, an increase in the electrophilic character of the carbonyl group by π–π stacking interaction of the phenyl group with organic ligand in CuBTC is expected.

Finally, we performed the condensation of 2-amino-4-chlorobenzonitrile **16** with **4** in a modified Friedländer reaction leading to substituted 4-aminoquinolines (Schemes 3 and 4). This condensation is often useful for the synthesis of compounds with pharmacological activity.[37] Thus, the reaction of **16** with **4**, under solvent free conditions, at 363 K, catalyzed by CuBTC afforded quinoline **17** with 39% yield after 5 h, with only traces of compound **18** being detected by MS. Compound **18** was formed by hydrolysis from the intermediate **19** (Table 5; entry 1). In order to increase the yield for compound **17** we

Table 5 Friedländer reaction between 2-amino-4-chlorobenzonitrile **16** and ketones catalyzed by CuBTC

Entry	*T*/°C	Time (h)	Yield of **20a** (%)	Yield of **20b** (%)
1	90	5	39[a]	—
2	100	4	83	—
3	100	5	58	42
4	100	5	49	51

Experimental conditions: 2-amino-4-chlorobenzonitrile 1 (0.5 mmol), acetylacetone 2 (5 mmol) and CuBTC was heated at the corresponding temperature during the time shown in table. [a] Traces of 18 (2%) were detected by ^{1}H-NMR and MS.

carried out the reaction at 373 K and duration 4 h leading to the corresponding quinoline in 83% yield. (Table 5; entry 2). We have also investigated the synthesis of 9-chloroacridine **20a** because it is a useful building block for the synthesis of acetylcholine esterase inhibitors.[38] The reaction of **16** with cyclohexanone (**6**) (at 373 K for 5 h) over CuBTC led to a mixture of products being identified as compounds **20a** (58%) and **20b** (42%), respectively (Scheme 4, Table 4; entry 3). Li *et al.*[39] reported this condensation employing stoichiometric $ZnCl_2$ amounts, in DMF at reflux, isolating compound **20b** as a major product. The formation of compound **20b** was rationalized as occurring first through a Pinner reaction and a subsequent Dimroth rearrangement. The CuBTC reported here appears as a new catalyst for this process, operating under milder reaction conditions and in a solvent-free environment, affording compounds **20a–b** in a 3 : 2 ratio.

We also carried out this reaction in the presence of $Cu(NO_3)_2$ leading to compounds **20a** and **20b** in 49% and 51% yield, respectively, after 5 h of the reaction. These results are important for the following reasons, i) the reaction leading to compounds **20a–b** is a catalytic process when using CuBTC or $Cu(NO_3)_2$ as heterogeneous or homogeneous catalysts, respectively, and ii) using the catalysts above mentioned it is possible to obtain quinoline **20a** with increased yield and selectivity.

2.4. Mechanistic considerations.

A tentative mechanism for the Friedländer reaction has been also investigated computationally using 2-aminobenzaldehyde (**21**) and acetaldehyde (**22k**) (Scheme 5). Although the chemical behaviour of this type of carbonyl compound is slightly different to that for the corresponding ketones, aldehydes were the substrates of our choice for simplicity for the theoretical calculations. Friedländer condensations between compounds **21** and **22k** could take place following two different effective pathways for

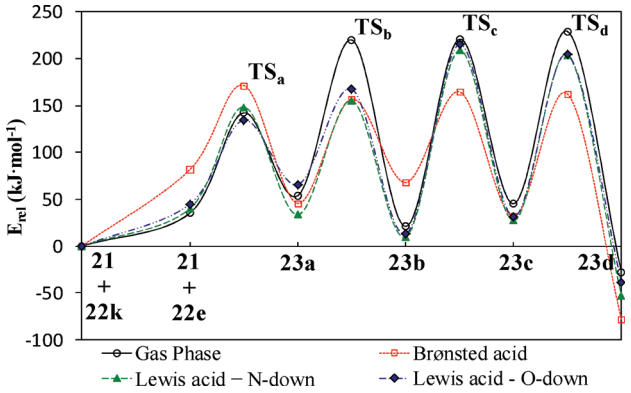

Fig. 8 Energy profile of Friedländer reaction between 2-aminobenzaldehyde (**21**) and acetaldehyde (**22**) following the reaction path starting with the aldolization step (Scheme 5). B3LYP energies calculated for uncatalyzed and catalyzed reactions are reported.

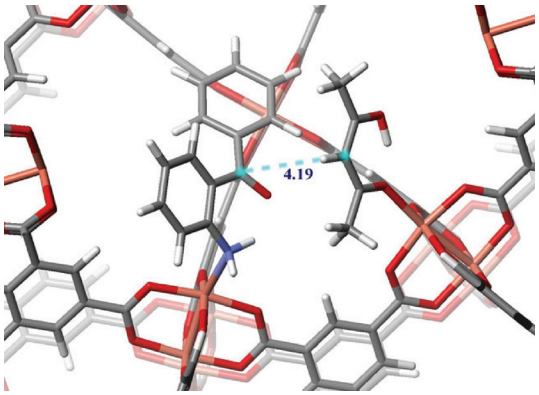

Fig. 9 Adsorption complex of CuBTC with reactants **3b** and **4** interacting with adjacent Cu^{2+} *cus* sites. Distance between atoms reacting in the first aldolization step is depicted (in Å). The following colouring scheme is adopted: Cu – orange, O – red, C – grey, N – blue, H – white.

the first reaction step i) aldolic condensation and ii) imination. Both of them were investigated, aldolic condensation being found to be energetically more favourable than the initial imine formation; therefore, only the aldolization mechanism is discussed below. Stationary points on the reaction path obtained at the B3LYP level for model reactants **21** and **22** are shown in Fig. 8 for the following situations: gas phase reaction, Brønsted acid catalysed (proton) reaction, and Lewis acid catalysed (CuBTC cluster model) reaction. It is apparent that Brønsted acid catalyst is the most efficient one, lowering barriers TS_b, TS_c, and TS_d by about 60 kJ mol^{-1}. The same catalytic effect is also found for the Lewis acid catalyst (CuBTC), however, only for the second reaction step (up to the ring closer, **23b**). The barriers for dehydration are lowered (with respect to the uncatalysed process) only by 5–25 kJ mol^{-1}. It should be pointed out that this small decrease in the barriers TS_c and TS_d can be due to a small cluster model used to mimic the active site (see Section 3.5.).

The purely energetic consideration presented above lead to the conclusions that Brønsted acid catalysts should be more efficient than Lewis acid ones. However, there is an additional, rather peculiar, effect of CuBTC that should not be overlooked: there is a large concentration of active sites in CuBTC (separated just by 8.15 Å) that can act in a concerted manner. In order to further increase our mechanistic understanding of the reactions investigated here experimentally, the interaction of reactants 2-aminobenzophenone (**3b**) and acetylacetone (**4**) with CuBTC represented by a periodic model was investigated. Both, 2-aminobenzophenone and acetylacetone interact preferentially with the Cu *cus* site (Fig. 9); the adsorption complexes *via* N- and O- atoms are practically isoenergetic ($-\Delta E_{ads}$ = 39 kJ mol^{-1}) in the case of 2-aminobenzophenone **3b**. The most stable adsorption complex of acetylacetone **4**, characterized by $-\Delta E_{ads}$ = 38 kJ mol^{-1}, is in its enol form (Fig. 9).

Considering the situation when reactants **3b** and **4** interact with adjacent *cus* sites, there are three possible arrangements of reactants, all of them having the same energy ($-\Delta E_{ads}$(**3b** + **4**) = 79 kJ mol^{-1}). One of the situations is depicted in Fig. 9; 2-aminobenzophenone **3b** interacts with *cus via* the N atom and acetylacetone **4** in its enol form interacts with neighboring *cus via* the O atom. Note that both reactants are ideally arranged for aldolization, the distance between reacting atoms (carbonyl carbon of **3b** and central carbon of **4**) is only 4.19 Å and mutual arrangement of the two reactants is such that the reaction can proceed without any steric hindrance. Similarly in the other two energetically preferable arrangements of **3b** and **4** on adjacent *cus* sites the orientation of reactants is favourable for the reaction.

Calculations on the periodic model of CuBTC thus show that the concerted effect of a pair of neighboring Cu^{2+} sites in CuBTC enhances the catalytic effect compared to an isolated Cu^{2+} Lewis acid center. The arrangement of reactants on neighboring *cus* sites described above should result in an increase in the pre-exponential factor of the reaction rate constant. In addition, close proximity of active *cus* sites may lead to a further decrease of TS_c and TS_d barriers due to the stabilization effect of the secondary Cu^{2+} site interacting with the produced water molecule.

It should be also pointed out that the formation of Brønsted acid sites by water adsorbed on Cr^{3+} sites in MIL-100 was reported.[40a] However, the involvement of similar Brønsted acid sites in CuBTC in the reaction investigated here is not likely. The Brønsted site formed in MIL-100(Cr) is significantly weaker than the Brønsted sites in H-zeolites (a shift of OH stretching frequency of −200 and −300 cm^{-1} was reported for MIL-100(Cr)

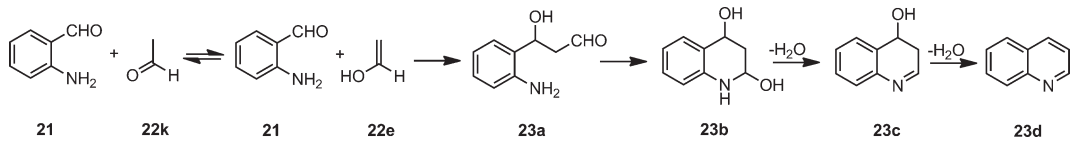

Scheme 5 Friedländer reaction between 2-aminobenzaldehyde (**21**) and acetaldehyde (**22**, k = keto form; e = enol form) – reaction path starting with aldolization step.

and, *e.g.*, H-FER,[40b] respectively) and the corresponding Brønsted site formed by water adsorbed on Cu^{2+} is even weaker. Calculated interaction energies for the second water molecule with the $H_2O\cdots Cu$ in CuBTC is less than 50 kJ mol^{-1}, significantly less than interaction energy of water with Brønsted sites in zeolites. IR data also suggest that there is no interaction with Brønsted centres in CuBTC, as proposed by Alaerts *et al.*[40c] The wide band of H_2O around 3300 cm^{-1} does not decrease after pyridine introduction, which proves that water is not replaced by pyridine. Additionally, the binding energy of the pair pyridine + H_2O was calculated by Watanabe and Sholl[41] as 0.2 eV, exactly the same as for the pair of H_2O molecules, therefore it is also unlikely that pyridine would replace water in the coordination sphere of Cu^{2+}.

3. Experimental

3.1. Specific surface area measurements

The surface area and void volumes of the zeolites under study were determined from adsorption isotherms of nitrogen at 77 K applying the BET method using a static volumetric apparatus Micromeritics, ASAP 2020 (Table 1).

3.2. Acidity in MOFs

The properties of CuBTC were investigated by adsorption of pyridine and carbon monoxide as a probe molecule followed by FTIR spectroscopy. CuBTC was prepared as self-supported wafers and activated as described in the text prior to the adsorption of probe molecules. The adsorption temperatures were 373 K for pyridine (POCh Gliwice, analytical grade, dried over 3A molecular sieve) and 173 K for CO (Linde Gas Polska, 99.5% used without further purification).

IR spectra were recorded with a Bruker Tensor 27 spectrometer equipped with an MCT detector and working with the spectral resolution of 2 cm^{-1}. All spectra presented in this work are normalized to the standard 10 mg pellet (density 3.2 mg cm^{-2}).

3.3. Product charaterization

NMR spectra were recorded with a Varian Mercury 300 spectrometer. ^1H chemical shifts (δ) in $CDCl_3$ are given using internal tetramethylsilane as the internal standard. MS spectra were recorded with a GS/MS ThermoElectron.

TLC chromatography was performed on DC-Aulofolien/Kieselgel 60 F_{245} (Merck) using mixtures of hexane/AcOEt or CH_2Cl_2/EtOH as eluents.

All reagents and solvents for catalytic studies were obtained from Aldrich. MOFs under study, CuBTC and FeBTC, were also commercially available.

3.4. Experimental procedures

3.4.1. Synthesis of 1-(6-chloro-2-methyl-4-phenyl-quinolin-3-yl)-ethanone (1b). To a mixture of the acetylacetone (**4**) (5 mmol) and activated CuBTC (0.083 mmol, 50 mg), 5-chloro-2-amino benzophenone (**3a**) (1 mmol) was added and the reaction mixture was heated at 363 K, for 2 h. The reaction was followed until total consumption of the starting material detected by TLC (mixture of EtOAc/*n*-hexane in 1 : 2 ratio was used as eluent). After cooling, reaction crude was treated with EtOH (96%) and the catalyst was removed by centrifugation at 4000 rpm for 10 min. Finally, solvent was removed under vacuum. Conversions were determined by ^1H NMR.

1-(6-Chloro-2-methyl-4-phenyl-quinolin-3-yl)-ethanone (**1b**). ^1H NMR (300 MHz, $CDCl_3$): δ 8.01 (1H, d J = 8.7 Hz), 7.65 (1H, dd J = 2.4, 9.0 Hz), 7.58–7.41 (4H, m), 7.37–7.31 (2H, m), 2.68 (3H, s), 2.00 (3H, s); MS (EI) *m*/*z* (%) 297(14), 296 (6), 295 (M^+, 44), 280 (100), 252 (21), 217 (52), 176 (47), 43 (61), 18 (87).

1-(2-Methyl-4-phenyl-quinolin-3-yl)-ethanone (**5**). ^1H NMR (300 MHz, $CDCl_3$): δ 8.08 (1H, d J = 8.1 Hz), 7.72 (1H, app t J = 6.9, 7.8 Hz), 7.62 (1H, d J = 8.1 Hz), 7.52–7.49 (3H, m), 7.48–7.42 (1H, m), 7.37–7.34 (2H, m), 2.70 (3H, s), 2.00 (3H, s); MS (EI) *m*/*z* (%) 261 (M^+, 42), 246 (100), 218 (61), 176 (41), 151 (20), 108 (18), 43 (28).

7-Chloro-9-phenyl-1,2,3,4-tetrahydro-acridine (**7**). ^1H NMR (300 MHz, $CDCl_3$): δ 7.98 (1H, d J = 8.7 Hz), 7.57–7.49 (5H, m), 2.28 (1H, d J = 1.8 Hz), 7.21 (1H, d J = 1.8, 8.1 Hz), 3.19 (2H, app t J = 6.3, 6.6 Hz), 2.59 (2H, app t J = 6.3, 6.6 Hz), 2.00–1.92 (2H, m), 1.82–1.72 (2H, m); MS (EI) *m*/*z* (%) 295 (36), 294 (32), 293 (M^+, 100), 292 (40), 258 (82), 120 (45).

7-Chloro-3,3-dimethyl-9-phenyl-3,4-dihydro-2*H*-acridin-1-one (**9**). ^1H NMR (300 MHz, $CDCl_3$): δ 8.00 (1H, d J = 0 9 Hz), 7.69 (1H, dd J = 2.1, 9 Hz), 7.53–7.42 (3H, m), 7.46 (1H, d J = 2.1 Hz), 7.17–7.14 (2H, m), 3.25 (2H, s), 2.57 (2H, s), 1.15 (6H, s). MS (EI) *m*/*z* (%) 338 (4), 337 (26), 336 (37), 335 (M^+, 76), 334 (M+-1, 90), 279 (55), 216 (100), 189 (33), 120 (36).

6-Chloro-2,4-diphenyl-quinoline (**11**). ^1H NMR (300 MHz, $CDCl_3$): δ 8.18 (2H, d J = 8.4 Hz), 7.86 (1H, d J = 7.5 Hz), 7.65–7.40 (11H, m); MS (EI) *m*/*z* (%) 317 (30), 316 (45), 315 (M^+, 92), 314 (93), 280 (41), 139 (100).

1-(6-Chloro-2,4-dimethyl-quinolin-3-yl)-ethanone (**15**). ^1H NMR (300 MHz, $CDCl_3$): δ 8.00 (2H, m), 7.70 (1H, d J = 8.1 Hz), 7.56 (1H, m), 2.63 (3H, s), 2.59 (3H, s), 2.58 (3H, s); MS (EI) *m*/*z* (%) 199 (M^+, 42), 184 (86), 156 (100), 115 (47), 43 (34).

1-(4-Amino-7-chloro-2-methyl-quinolin-3-yl)-ethanone (**17**). ^1H NMR (300 MHz, $CDCl_3$): δ 12.68 (2H, s), 7.85 (1H, d J = 7.8 Hz), 7.66 (1H, s), 7.40 (1H, d J = 7.8 Hz), 5.45 (1H, s), 2.06 (3H, s), 2.04 (3H, s); MS (EI) *m*/*z* (%) 234 (M^+, 11), 219 (39), 43 (100);. 1-(7-Chloro-4-hydroxy-2-methyl-quinolin-3-yl)-ethanone (**18**). MS (EI) *m*/*z* (%)234 (M^+-1, 33), 219 (53), 18 (100).

6-Chloro-1,2,3,4-tetrahydro-acridin-9-ylamine (**20a**). ^1H NMR (300 MHz, DMSO-d_6): δ 8.18 (1H, d J = 9 Hz), 7.62 (1H, d J = 1.8 Hz), 7.28 (1H, dd J = 9, 1.8 Hz), 6.51 (2H, br s), 2.8 (2H, m), 2.58 (2H, m), 1.81-1.65 (4H, m).

6-Chloro-2,2-pentamethylene-1,2-dihydroquinazolin-4(3*H*)-one (**20b**). ^1H NMR (300 MHz, $CDCl_3$): δ 8.08 (1H, s), 7.54 (1H, d J = 8.1 Hz), 6.93 (1H, s), 6.87 (1H, d J = 2.1 Hz), 6.62 (1H, dd J = 8.1, 2.1 Hz), 1.71–1.23 (10H, m).

Catalyst activation: CuBTC was dried, at 373 K, overnight (experimental conditions: 373 K, 5 K min^{-1}, 900 min).

Spectroscopic data of compounds **1b**,[25] **5**, **7–11**,[25,42] **15**[42] and **20**[39] are in accordance with those reported.

3.5. Theoretical calculations

The mechanism of the Friedländer reaction taking place in a gas phase without any catalyst, the reaction catalyzed by Brønsted acid (H^+ ions) and the reaction catalyzed by Lewis acid (Cu^{2+} ions) was investigated using cluster models and Becke's three parameter exchange–correlation functional B3LYP[43,44] together with 6-311G(2d,p) basis set.[45] The active site in CuBTC MOF was represented by the $Cu(HCOO)_2$ cluster constrained at the geometry obtained for $Cu_2(HCOO)_4$ paddlewheel. Character of all stationary points located along the reaction path was checked by the frequency calculations performed within the harmonic approximation. All energies were corrected for zero-point-vibrational energy correction. Cluster model calculations were performed with Gaussian09 program suite.[46]

The Friedländer reaction taking place in CuBTC was further investigated with the periodic DFT model, employing the PBE functional.[47] The periodic DFT calculations were performed for the ferromagnetic case, using the rhombohedral primitive cell containing 156 framework atoms (12 Cu^{2+} cations) and cell parameters optimized previously ($a = b = c = 18.774$ Å and $\alpha = \beta = \gamma = 60°$).[48] The projector augmented wave (PAW)[49] and kinetic energy cutoff of 600 eV were used together with the Γ-point sampling of the first Brillouin zone. Periodic DFT calculations were performed with VASP 5.2 package.[50,51] It has been shown recently that interaction of adsorbate with *cus* sites in CuBTC is underestimated at the DFT level[48] due to the lack of dispersion interaction and due to the description of the Cu^{2+} site and, therefore, they should be considered as qualitative. Nevertheless, this error is expected to be very similar for all structures reported here, thus, relative energies should not be strongly affected.

4. Conclusions

Textural and acid properties of commercial CuBTC were characterized in this study. In particular, their catalytic performance in the condensation of 2-aminoaryl ketones or 2-amino-4-chlorobenzonitrile with different ketones was evaluated. The reaction takes place under solvent-free conditions and it proceeds with good efficiency and selectivity; therefore, CuBTC investigated here was identified as promising heterogeneous catalyst for this and similar condensations.

The catalytic activity of CuBTC was also compared with the activity of H-BEA, Cu-BEA and (Al)SBA-15 materials and experimental investigation was accompanied by the DFT modelling of the reaction mechanisms catalyzed by Brønsted and Lewis acid centers. Two effects of MOF catalysts on the course of the Friedländer reaction were identified: (i) lowering of energy barriers, especially for the annulation reaction step and (ii) favourable geometry of the reaction precursor formed by adsorption of reactants on two adjacent Cu^{2+} sites in CuBTC. High concentration of the active sites in CuBTC (compared with H-BEA or Cu-BEA) together with the concerted effect of two adjacent active sites is behind a very high catalytic activity of these MOF materials for the reactions investigated here.

Among several reactions discussed, it was also shown that the CuBTC is an interesting heterogeneous catalyst for the preparation of 9-chloroacridine, an important intermediate in the preparation of AchE inhibitors *via* a modified Friedländer reaction.

Acknowledgements

The research leading to these results has received funding from the European Community's Seventh Framework Programme (FP7/2007-2013) under grant agreement n° 228862. MACADEMIA is a Large-scale Integrating Project under the Nanosciences, Nanotechnologies, Materials and New Production Technologies Theme (www.macademia-project.eu). PN and MP also acknowledge the support of ME CR (grants 7E09111 and MSM0021620857). This work has been also supported by MICINN (CTQ2009-10478). The IR studies were carried out with the equipment purchased thanks to the financial support of the European Regional Development Fund in the framework of the Polish Innovation Economy Operational Program (contract no. POIG.02.01.00-12-023/08).

References

1 F. X. L. I. Xamena, A. Corma and H. Garcia, *J. Phys. Chem. C*, 2007, **111**, 80–85.
2 D. Zacher, O. Shekhah, C. Woll and R. A. Fischer, *Chem. Soc. Rev.*, 2009, **38**, 1418–1429; B. V. Harbuzaru, A. Corma, F. Rey, J. L. Jorda, D. Ananias, L. D. Carlos and J. Rocha, *Angew. Chem., Int. Ed.*, 2009, **48**, 6476–6479; M. Dan-Hardi, C. Serre, T. Frot, L. Rozes, G. Maurin, C. Sanchez and G. Ferey, *J. Am. Chem. Soc.*, 2009, **131**, 10857–10859; B. V. Harbuzaru, A. Corma, F. Rey, P. Atienzar, J. L. Jorda, H. García, D. Ananias, L. D. Carlos and J. Rocha, *Angew. Chem., Int. Ed.*, 2008, **47**, 1080–1083.
3 S. Q. Ma and H. C. Zhou, *Chem. Commun.*, 2010, **46**, 44–53; J. R. Li, R. J. Kuppler and H. C. Zhou, *Chem. Soc. Rev.*, 2009, **38**, 1477–1504; M. P. Suh, Y. E. Cheon and E. Y. Lee, *Coord. Chem. Rev.*, 2008, **252**, 1007–1026.
4 S. M. Cohen, *Curr. Opin. Chem. Biol.*, 2007, **11**, 115–120.
5 A. Corma, H. García, F. X. Llabrés and I. Xamena, *Chem. Rev.*, 2010, **110**, 4606–4655; V. I. Isaeva and L. M. Kustov, *Pet. Chem.*, 2010, **50**, 167–180.
6 M. Bejblova, D. Prochazkova and J. Čejka, *ChemSusChem*, 2009, **2**, 486–499; A Bhan and E. Iglesia, *Acc. Chem. Res.*, 2008, **41**, 559–567; A. Corma, *J. Catal.*, 2003, **216**, 298–312.
7 J. Y. Lee, O. K. Farha, J. Roberts, K. A. Scheidt, S. B. T. Nguyen and J. T. Hupp, *Chem. Soc. Rev.*, 2009, **38**, 1450–1459; D. Farrusseng, S. Aguado and C. Pinel, *Angew. Chem., Int. Ed.*, 2009, **48**, 7502–7513.
8 Y. Wu, L.-G. Qiu, W. Wang, Z.-Q. Li, T. Xu, Z.-Y. Wu and X. Jiang, *Transition Met. Chem.*, 2009, **34**, 263–268.
9 A. Dhakshinamoorthy, M. Alvaro and H. Garcia, *J. Catal.*, 2009, **267**, 1–4.
10 Y.-K. Seo, G. Hundal, I. T. Jang, Y. K. Hwang, C.-H. Jun and J.-S. Chang, *Microporous Mesoporous Mater.*, 2009, **119**, 331–337; S. S.-Y. Chui, S. M. F. Lo, J. P. H. Charmant, A. G. Orpen and I. D. Williams, *Science*, 1999, **283**, 1148–1150.
11 L. Alaerts, E. Séguin, H. Poelman, F. Thibault-Starzyk, P. A. Jacobs and D. E. De Vos, *Chem.–Eur. J.*, 2006, **12**, 7353–7363.
12 K. Schlichte, T. Kratzke and S. Kaskel, *Microporous Mesoporous Mater.*, 2004, **73**, 81–88.
13 A. Corma, M. Iglesias, F. X. L. I Xamena and F. Sanchez, *Chem.–Eur. J.*, 2010, **16**, 9789–9795.
14 E. Pérez-Mayoral and J. Čejka, *ChemCatChem*, 2011, **3**, 157–159.
15 J. López-Sanz, E. Pérez-Mayoral, D. Procházková, R. M. Martín-Aranda and A. J. López-Peinado, *Top. Catal.*, 2010, **53**, 1430–1437.
16 J. Marco-Contelles, E. Pérez-Mayoral, A. Samadi, M. do Carmo Carreiras and E. Soriano, *Chem. Rev.*, 2009, **109**, 2652–2671.
17 J. Akbari, A. Heydari, H. R. Kalhor and S. A. Kohan, *J. Comb. Chem.*, 2010, **12**, 137–140; D. Garella, A. Barge, D. Upadhyaya, Z. Rodriguez, G. Palmisano and G. Cravotto, *Synth. Commun.*, 2010, **40**, 120–128; R. M. Martin-Aranda and J. Čejka, *Top. Catal.*, 2010, **53**, 141–153.

18 G. C. Muscia, M. Bollini, J. P. Carnevale, A. M. Bruno and S. E. Asís, *Tetrahedron Lett.*, 2006, **47**, 8811–8815.
19 I. Dorronsoro, D. Alonso, A. Castro, M. del Montea, E. García-Palomero and A. Martínez, *Arch. Pharm.*, 2005, **338**, 18–23.
20 K. Mogilaiah and K. Vidya, *Indian J. Chem. B*, 2007, **46B**, 1721–1723.
21 A. Shaabani, E. Soleimani and Z. Badri, *Monatsh. Chem.*, 2006, **137**, 181–184.
22 M. A. Zolfigol, P. Salehi, M. Shiri, T. F. Rastegar and A. Ghaderi, *J. Iran. Chem. Soc.*, 2008, **5**, 490–497.
23 B. Das, K. Damodar, N. Chowdhury and R. A. Kumar, *J. Mol. Catal. A: Chem.*, 2007, **274**, 148–152.
24 M. Dabiri, S. C. Azimi and A. Bazgir, *Monatsh. Chem.*, 2007, **138**, 659–661.
25 U. V. Desai, S. D. Mitragotri, T. S. Thopate, D. M. Pore and P. P. Wadgaonkar, *Arkivoc*, 2006, **xv**, 198–204.
26 M. Narasimhulu, T. S. Reddy, K. C. Mahesh, P. Prabhakar, Ch. B. Rao and Y. Venkateswarlu, *J. Mol. Catal. A: Chem.*, 2007, **266**, 114–117.
27 B. Das, M. Krishnaiah, K. Laxminarayana and D. Nandankumar, *Chem. Pharm. Bull.*, 2008, **56**, 1049–1051.
28 A. A. Mohammadi, J. Azizian, A. Hadadzahmatkesh and M. R. Asghariganjeh, *Heterocycles*, 2008, **75**, 947–954.
29 A. Shaabani, A. Rahmati and Z. Badri, *Catal. Commun.*, 2008, **9**, 13–16.
30 D. Garella, A. Barge, D. Upadhyaya, Z. Rodriguez, G. Palmisano and G. Cravotto, *Synth. Commun.*, 2010, **40**, 120–128.
31 S. Chauhan, R. Chakravarti, S. M. J. Zaidi, S. S. Aldeyab, V. Basireddy and A. Vinu, *Synlett*, 2010, **17**, 2597–2600.
32 F. Domínguez-Fernández, J. López-Sanz, E. Pérez-Mayoral, D. Bek, R. M. Martín-Aranda, A. J. López-Peinado and J. Cejka, *ChemCatChem*, 2009, **1**, 241–243.
33 R. Brosius, D. Gammon, F. Van Laar, E. van Steen, B. Sels and P. Jacobs, *J. Catal.*, 2006, **239**, 362–368.
34 F. Watari and S. Kinumaki, *Sci. Rep. RITU A*, 1962, **14**, 64; I. S. Perelygin and M. A. Klimchuk, *Zhournal Prikladnoi Spectroskopii*, 1976, **24**, 65; R. Ferwerda, J. H. van der Maas and F. B. van Duijnevelt, *J. Mol. Catal. A: Chem.*, 1996, **104**, 319–328.
35 A. Dandekar and M. A. Vannice, *J. Catal.*, 1998, **178**, 621–639.
36 G. Busca, *J. Mol. Catal.*, 1987, **43**, 225.
37 M. L. Bolognesi, M. Bartolini, F. Mancini, G. Chiriano, L. Ceccarini, M. Rosini, A. Milelli, V. Tumiatti, V. Andrisano and C. Melchiorre, *ChemMedChem*, 2010, **5**, 1215–1220; M. Incerti, L. Flammini, F. Saccani, G. Morini, M. Comini, M. Coruzzi, E. Barocelli, V. Ballabeni and S. Bertoni, *ChemMedChem*, 2010, **5**, 1143–1149; M. I. Fernandez-Bachiller, C. Perez, G. C. Gonzalez-Munoz, S. Conde, M. G. Lopez, M. Villarroya, A. G. Garcia and M. I. Rodriguez-Franco, *J. Med. Chem.*, 2010, **53**, 4927–4937.
38 P. Camps, X. Formosa, D. Muñoz-Torrero, J. Petrignet, A. Badia and M. V. Clos, *J. Med. Chem.*, 2005, **48**, 1701–1704; V. Tumiatti, A. Minarini, M. L. Bolognesi, A. Milelli, M. Rosini and C. Melchiorre, *Curr. Med. Chem.*, 2010, **17**, 1825–1838.
39 J. Li, L. Zhang, D. Shi, Q. Li, D. Wang, Ch. Wang, Q. Zhang, L. Zhang and Y. Fan, *Synlett*, 2008, **2**, 233–236.
40 (*a*) A. Vimont, J. M. Goupil, J. C. Lavalley, M. Daturi, S. Surble, C. Serre, F. Millange, G. Ferey and N. Audebrand, *J. Am. Chem. Soc.*, 2006, **128**, 3218–3227; (*b*) P. Nachtigall, O. Bludsky, L. Grajciar, D. Nachtigallova, M. R. Delgado and C. O. Arean, *Phys. Chem. Chem. Phys.*, 2009, **11**, 791–802; (*c*) L. Alaerts, E. Seguin, H. Poelman, F. Thibault-Starzyk, P. A. Jacobs and D. E. De Vos, *Chem.–Eur. J.*, 2006, **12**, 7353–7363.
41 T. Watanabe and D. S. Sholl, *J. Chem. Phys.*, 2010, **133**, 094509.
42 L. Wu, C. Yang, B. Niu and F. Yan, *Monatsh. Chem.*, 2009, **140**, 1195–1198; S. S. Palimkar, S. A. Siddiqui, T. Daniel, R. J. Lahoti and K. V. Srinivasan, *J. Org. Chem.*, 2003, **68**, 9371–9378.
43 A. D. Becke, *J. Chem. Phys.*, 1993, **98**, 5648–5652.
44 C. T. Lee, W. T. Yang and R. G. Parr, *Phys. Rev. B*, 1988, **37**, 785–789.
45 R. Krishnan, J. S. Binkley, R. Seeger and J. A. Pople, *J. Chem. Phys.*, 1980, **72**, 650–654.
46 M. J. Frisch, G. W. Trucks, H. B. Schlegel, G. E. Scuseria, M. A. Robb, J. R. Cheeseman, G. Scalmani, V. Barone, B. Mennucci, G. A. Petersson, H. Nakatsuji, M. Caricato, X. Li, H. P. Hratchian, A. F. Izmaylov, J. Bloino, G. Zheng, J. L. Sonnenberg, M. Hada, M. Ehara, K. Toyota, R. Fukuda, J. Hasegawa, M. Ishida, T. Nakajima, Y. Honda, O. Kitao, H. Nakai, T. Vreven, J. A. Montgomery, Jr., J. E. Peralta, F. Ogliaro, M. Bearpark, J. J. Heyd, E. Brothers, K. N. Kudin, V. N. Staroverov, R. Kobayashi, J. Normand, K. Raghavachari, A. Rendell, J. C. Burant, S. S. Iyengar, J. Tomasi, M. Cossi, N. Rega, J. M. Millam, M. Klene, J. E. Knox, J. B. Cross, V. Bakken, C. Adamo, J. Jaramillo, R. Gomperts, R. E. Stratmann, O. Yazyev, A. J. Austin, R. Cammi, C. Pomelli, J. Ochterski, R. L. Martin, K. Morokuma, V. G. Zakrzewski, G. A. Voth, P. Salvador, J. J. Dannenberg, S. Dapprich, A. D. Daniels, O. Farkas, J. B. Foresman, J. V. Ortiz, J. Cioslowski and D. J. Fox, *GAUSSIAN 09 (Revision A.1)*, Gaussian, Inc., Wallingford, CT, 2009
47 J. P. Perdew, K. Burke and M. Ernzerhof, *Phys. Rev. Lett.*, 1996, **77**, 3865–3868.
48 L. Grajciar, O. Bludsky and P. Nachtigall, *J. Phys. Chem. Lett.*, 2010, **1**, 3354–3359; L. Grajciar, A. D. Wiersum, P. Llewellyn, J. S. Chang and P. Nachtigall, *J. Phys. Chem. C*, 2011, **115**, 17925.
49 P. E. Blochl, *Phys. Rev. B: Condens. Matter*, 1994, **50**, 17953–17979.
50 G. Kresse and J. Hafner, *Phys. Rev. B: Condens. Matter*, 1993, **48**, 13115–13118.
51 G. Kresse and D. Joubert, *Phys. Rev. B: Condens. Matter Mater. Phys.*, 1999, **59**, 1758–1775.

